Spin-Polarized Transport and Dynamics in Magnetic Tunneling Structures

R. Cao[1], T. Moriyama[1], W. G. Wang[1], X. Fan[1], J. Kolodzey[2], S. H. Chen[1,3], C. R. Chang[3], Y. Tserkovnyak[4], B. K. Nikolic[1], and J. Q. Xiao[1]

[1]Department of Physics and Astronomy, University of Delaware, Newark, DE 19716 USA
[2]Department of Electrical and Computer Engineering, University of Delaware, Newark, DE 19716 USA
[3]Department of Physics, National Taiwan University, Taipei 10617, Taiwan
[4]Department of Physics and Astronomy, University of California, Los Angeles, CA 90095 USA

In the first part of this paper, we report a systematic study on the structural evolution under rapid thermal annealing and the corresponding transport properties in magnetic tunnel junctions (MTJs) with a crystalline MgO barrier. The results clearly indicate that high tunneling magnetic resistance can be achieved by annealing MTJs at a very short time, and it is directly related to the formation of (001) crystalline structures. In the second part, we report the spin dynamics in tunneling structure through direct electrical detection. A surprisingly large voltage generation in $F/I/N$ and $F/I/F$ junctions was observed, which is contradictory to the prediction from the standard spin-pumping theory. We proposed a theoretical formalism to study spin-pumping effects in ferromagnetic multilayer structures. The formalism can yield a remarkably clean physical picture of the spin and charge pumping in tunneling structures. The calculated values are consistent with experimental results.

Index Terms—**Magnetic tunneling junction (MTJ), spin dynamics, transport.**

SPINTRONICS has attracted enormous scientific and technological attentions since the discovery of giant magnetoresistance (GMR) effects in 1988 [1], [2] by Fert and Grünberg who were awarded the 2007 Nobel Prize in physics. The influence of spin on the electric conduction in the ferromagnetic heterostructures establishes the cornerstone for spintronics. The goal of spintronics is to effectively generate spin current, control its transport across the interfaces and materials, and develop means of detection. Success in all these aspects will lead to new multifunctional devices offering nonvolatility, higher processing speeds, higher packing densities, and reduced power consumption. One good example is spin-polarized light-emitting diode (LED) that emits left or right circularly polarized light by injecting spin-polarized electrons (or holes) [3]. Most spintronic devices can be categorized in metal and semiconductor-based structures. The metallic spintronic devices evolve from simple spin valve (SV)-type structures to magnetic tunnel junctions (MTJs) based on amorphous Al_2O_3 barriers, and more recently based on crystalline MgO barriers. Many interesting physics exist in MTJ structures including, for example, Kondo effect, spin-orbital interaction, band structure, and spin current generation [4]–[7]. MTJs have found wide applications as biosensors, computer hard disk read heads, magnetic random access memory (MRAM), and microwave oscillators [8]–[13]. The central unit of an MTJ consists of two ferromagnetic layers separated by a nanometer-thick insulating barrier layer. One of the key features of MTJs is that the tunneling conductance depends on the relative angle between the magnetizations of two ferromagnetic layers, which can be modulated by the external magnetic field. This feature gives rise to tunneling magnetoresistance (TMR), which actually was first reported in Julliere's work more than 30 years ago [14]. TMR phenomenon arises from the fact that the electron tunneling probability depends on spin because of the different wave vectors at Fermi level for spin-up and spin-down electrons due to the exchange splitting in ferromagnetic materials.

While most static features in MTJs have been understood, the properties related with spin dynamics remain elusive. The demand of high-speed spintronic devices requires the working frequency to gigahertz range that is close to the characteristic precessing frequency (ferromagnetic resonant frequency) of magnetization in ferromagnetic materials. The discovery of new phenomena on high-frequency spin dynamics in MTJs opens new avenues to explore new physics and applications. One such new discovery is the spin-pumping effect, where the precessing magnetization of a ferromagnetic layer pumps spins into adjacent normal metallic layers without external direct current (dc) bias. An rf field is used to precess the magnetization under the ferromagnetic resonance. Spin-pumping effect is a promising candidate for realizing a spin battery device as a source for a pure spin current with no net charge current [15].

In this paper, we present our recent results on MTJs. Section I focuses on the structural evolution and related transport properties of MgO-based MTJs, which has not been systematically investigated and documented in the literature. What distinguishes this study from others is that, contrary to common 1–2-h postannealing treatment, we monitored the evolution of TMR in CoFeB/MgO/CoFeB MTJs through rapid annealing, resulting in fast crystallization of amorphous CoFeB electrodes. Our results show that the giant TMR could be established on a very short time scale. In Section II, we report our studies on spin dynamics in tunneling structures. We observed a surprisingly large dc voltage generated in $Al/AlO_x/Ni_{80}Fe_{20}/Cu$ $(F/I/N)$ structures from a precessing $Ni_{80}Fe_{20}$ layer, excited via an external rf field. The observed voltage is about an order of magnitude larger than the voltage observed in ohmic Cu/FeNi/Pt structures $(N/F/N)$ [16]. The results are abnormal if one considers that the spin-pumping effect is not expected in tunneling structures due to the negligibly small spin injection

Manuscript received March 06, 2009. Current version published September 18, 2009. Corresponding author: J. Q. Xiao (e-mail: jqx@udel.edu).
Color versions of one or more of the figures in this paper are available online at http://ieeexplore.ieee.org.
Digital Object Identifier 10.1109/TMAG.2009.2024126

0018-9464/$26.00 © 2009 IEEE

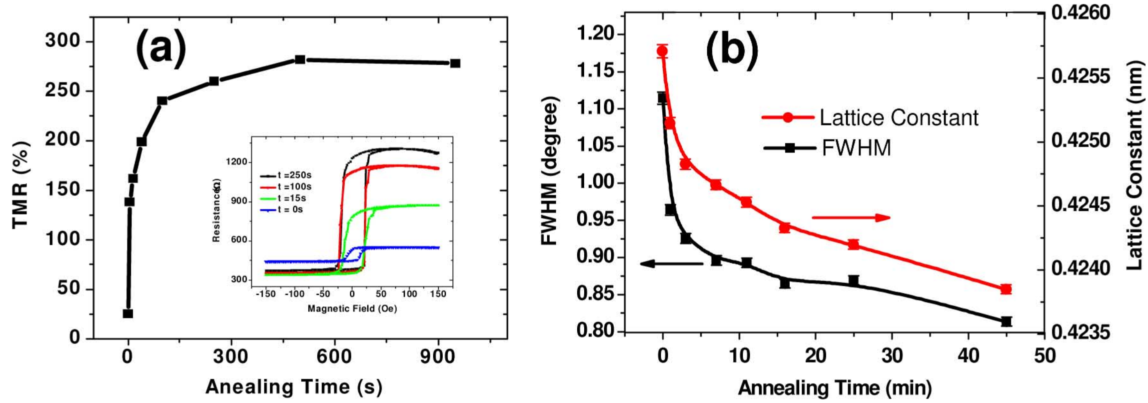

Fig. 1. (a) The evolution of TMR in CoFeB/MgO/CoFeB junctions during annealing at 460 °C. Inset shows the actual resistance versus the magnetic field at different annealing time durations. (b) The evolution of MgO barrier structure during annealing at 380 °C in the sample of Si/SiO_2/CoFeB 15/MgO 15/CoFeB 3.5/Ta 5. The FWHM of the MgO (002) XRD peak quickly decreases, accompanied by the fast change in lattice parameter at the beginning of the annealing.

rate, which is much smaller than the spin relaxation rate. Our results suggest a new nonequilibrium mechanism for the spin and charge pumping. More subtle physics have been revealed by the theoretical analyses regarding the spin and charge pumping [17], which appears to be very different from $N/F/N$ structures with ohmic interfaces. Moreover, in a recent study [18], we have introduced a novel theoretical formalism that is capable of addressing pumping problems in complicated heterostructures where the conventional approaches fail due to the spin accumulation not being well defined in an insulating layer. Both experimental and theoretical results will be discussed in Section II. Finally, we summarize our studies in Section III.

I. Structural Evolution and Spin-Polarized Transport in MgO-Based MTJs

It was predicted in 2001 that the TMR up to 1000% could be obtained in MTJs with crystalline MgO insulating barriers [19], [20]. In 2004, two groups independently reported giant TMR ratio close to 200% in MTJs consisting of crystalline MgO barriers [8], [9]. Up to date, the commonly used MTJ structure is CoFeB(001)/MgO(001)/CoFeB(001) junctions, where rf sputtered MgO layer has (001) texture on the as-deposited amorphous CoFeB layer. This (001)-oriented MgO layer serves as a supporting template for the crystallization of CoFeB layers during the postannealing process, which is commonly done above 350 °C for about 1–2 h. The final CoFeB/MgO/CoFeB with highly (001) texture provides the symmetry-conserved coherent tunneling, resulting in a giant TMR.

Unlike in AlO_x-based MTJs where annealing is only used to improve the TMR, the thermal annealing is an indispensable step to achieve a giant TMR in CoFeB/MgO/CoFeB junctions. It is because the coherent tunneling only occurs after as-deposited amorphous CoFeB layer crystallizes into (001) orientation. There are many studies on the effect of annealing temperature [10], [21]–[24], but none of them studies the dependence of TMR on the annealing time. The understanding of the TMR evolution during the annealing process is also very small, despite the fact that coherent tunneling theory can well explain the giant TMR in fully annealed samples [12], [19], [20]. Here, we report our recent studies on the real-time evolution of TMR during thermal annealing. We demonstrate that the TMR is quickly developed at the beginning of the annealing process and then followed by a slow approach to saturation.

The MgO tunneling junctions were fabricated in a magnetron sputtering system with a base pressure of 2×10^{-8} torr. The sample structure was Si/SiO_2/Ta 7/Ru 20/Ta 7/CoFe 2/IrMn 15/CoFe 2/Ru 1.7/CoFeB 3/MgO 1.8–3.2/CoFeB 3/Ta 8/Ru 10, where the numbers are layer thicknesses in nanometers. A wedged MgO barrier was deposited by a combinational technique. After the fabrication, the samples were then patterned into small sizes ranging from 5 to 100 μm by photolithography and ion-beam milling. In order to study the evolution of TMR in a very short time frame, a rapid thermal anneal (RTA) system was used to anneal the MTJs. For more details on the sample fabrication, refer to our previous publications [25]–[27].

Fig. 1(a) shows the evolution of TMR annealed at 460 °C. The data is obtained on the same sample at different length of accumulated annealing time. Both TMR and X-ray diffraction (XRD) measurements were performed right after the annealing, and then the processes were repeated for the different annealing time. During the annealing, the sample was cooled down under a magnetic field of 2 kOe in order to reestablish the exchange bias on FeCo layer since the annealing temperature is higher than the blocking temperature of the exchange bias. The sample was first heated up to 190 °C for a few seconds in a magnetic field of 600 Oe, in order to establish the exchange pinning. At this short annealing, referred to as "0 s," TMR is only 25%. TMR increases to around 140% by annealing the sample for 15 s at 460 °C and further increases to 240% after 100-s annealing. TMR approaches saturation after 300 s and then slowly decreases for annealing longer than 600 s. The TMR evolution during the annealing is clearly shown in the inset of Fig. 1(a), where the actual TMR curves were plotted as a function of the magnetic field. The results demonstrate that the development of TMR in CoFeB/MgO/CoFeB junctions occurs on an extremely short time scale compared to the traditional annealing time of 1 or 2 h. In order to correlate the structural information to spin-polarized transport properties, the evolution of MgO barrier structure during annealing at 380 °C was studied by performing an XRD experiment in a sample of Si/SiO_2/CoFeB 15/MgO 15/CoFeB 3.5/Ta 5, where the numbers are layer thicknesses

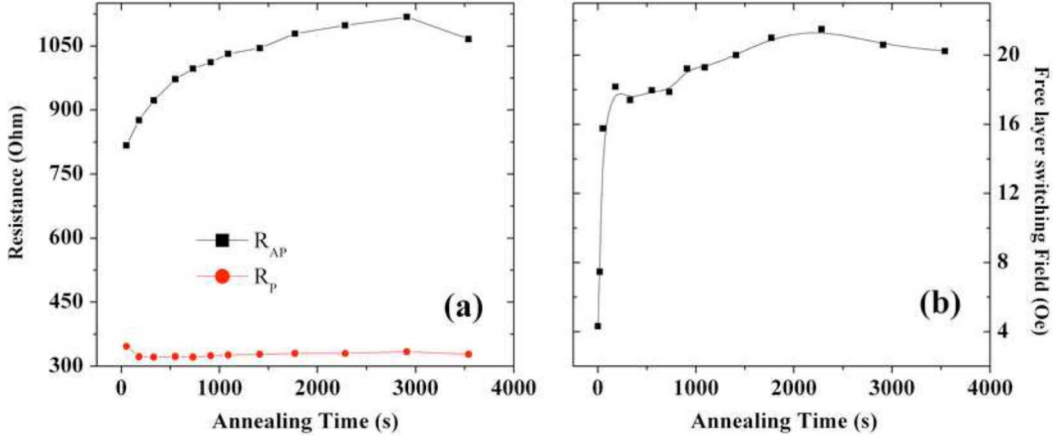

Fig. 2. (a) The annealing time dependence of R_{AP} and R_P of CoFeB/MgO/CoFeB junctions measured at room temperature. The samples were annealed at 380 °C. (b) The evolution of the switching field of free CoFeB electrode as a function of the annealing time.

in nanometers. We have to point out that the trends of the structure evolution are very similar at both 380 °C and 460 °C. The full-width at half maximum (FWHM) of the MgO (002) diffraction peak and the calculated lattice constant as a function of the annealing time are shown in Fig. 1(b). Both of them behave in the same manner, where a rapid drop is shown during the first few minutes of annealing and followed by a slow decreasing in prolonged annealing. Our results clearly indicate that the most structure evolution of CoFeB/MgO/CoFeB junction also happens at a short time scale of a few minutes during annealing.

The resistance changes during the annealing in parallel (R_P) and antiparallel (R_{AP}) states are plotted in Fig. 2(a). CoFeB/MgO/CoFeB junctions were annealed at 380 °C and the resistances were measured at room temperature. The quick increase of R_{AP} and the decrease of R_P are observed at the beginning of the annealing, similar to the TMR evolution and the lattice constant changes during the annealing. This is due to the coherent tunneling of the half-metallic and slow-decaying Δ_1 band, which depends on the crystalline structure of CoFeB electrodes and the magnetization states. The switching field of the free CoFeB layer also exhibits the similar dependence on the annealing time [Fig. 2(b)]. After only a few minutes of annealing, the switching field increases from 4 to 18 Oe. Then, it slowly approaches to saturation at longer annealing time.

All the results here indicate that the high values of TMR induced by the structural changes of CoFeB/MgO/CoFeB junctions occur at a very short time scale at high temperature. The highest TMR of 280% in our study is achieved in MTJs annealed for 6 min at 460 °C [28]. This discovery could be very useful for industry applications.

II. Spin Dynamics Study of MTJs

Although spin dynamics has been studied for a long time and the phenomenological Landau–Lifshitz–Gilbert equation describes many phenomena reasonably well, there are still many unanswered questions. For example, a complete theoretical description of the magnetic damping is still missing [29]. In 1996, Slonczewski [30] and Berger [31] predicted that the spin current flowing through magnetic multilayer could exerts a *spin-transfer torque* on the magnetization, leading to magnetization precession and even reversal if the current density was large enough. On the equal footing, the precessing magnetizations in a ferromagnet excited by an rf external field can inject spins into neighboring layers, giving rise to spin-pumping effect [32], [33]. Up to now, the spin-pumping effect was commonly demonstrated indirectly by observing enhanced Gilbert damping constant ferromagnetic/nonmagnetic layered systems [34], [35].

The spin injection into a nonmagnetic layer splits chemical potential between spin-up and spin-down electronic bands. This splitting, in principle, can be directly detected by a second ferromagnetic layer via a tunneling barrier. Depending on the relative orientation between the magnetization of the detecting ferromagnet and the spin accumulation in the normal metal, the observed voltages are expected to vary. The largest voltage difference $p\mu_s$ should be observed between parallel and antiparallel states, where p is the relative polarization of the spin-dependent tunnel conductance of the electrode and μ_s is the spin accumulation in the normal metal [33]

$$\mu_s = \hbar\omega \frac{\sin^2\theta}{\sin^2\theta + \eta} \tag{1}$$

where $\eta = \tau_i/\tau_{sf}$ is a reduction factor expressed in the ratio between the spin-flip rate and the spin injection rate. In a recent letter, Wang proposed a simple scheme to electrically measure the spin accumulation [36]. An F/N layer is used to convert pumped spin accumulation into a charge voltage. The single ferromagnet serves as both the source and the detector for spin-pumping current. The detection is realized by partially absorbing the back flow spin current through the spin flip scattering, thus generating a net charge voltage due to the spin-dependent interface and bulk conductance. Under the assumption that the layer thickness of the N layer is much smaller than its spin diffusion length, the voltage across the F/N interface is

$$V_{\rm dc} = \frac{p_\omega g_F \sin^2\theta\cos\theta}{(g_\omega - p_\omega^2 g_\omega + g_F)(\eta_N + \sin^2\theta) + (1-p_\omega^2) g_F \cos^2\theta g_\omega / g_\omega^{\uparrow\downarrow}} \times \frac{\hbar\omega}{2e} \tag{2}$$

where $\eta_N = g_N/g_\omega^{\uparrow\downarrow}\tanh(d_N/\lambda_{\rm sd}^N)$ with the thickness d_N and the spin diffusion length $\lambda_{\rm sd}^N$ of normal metal layer, g_F and g_N are the bulk conductance of FM and NM layer, respectively.

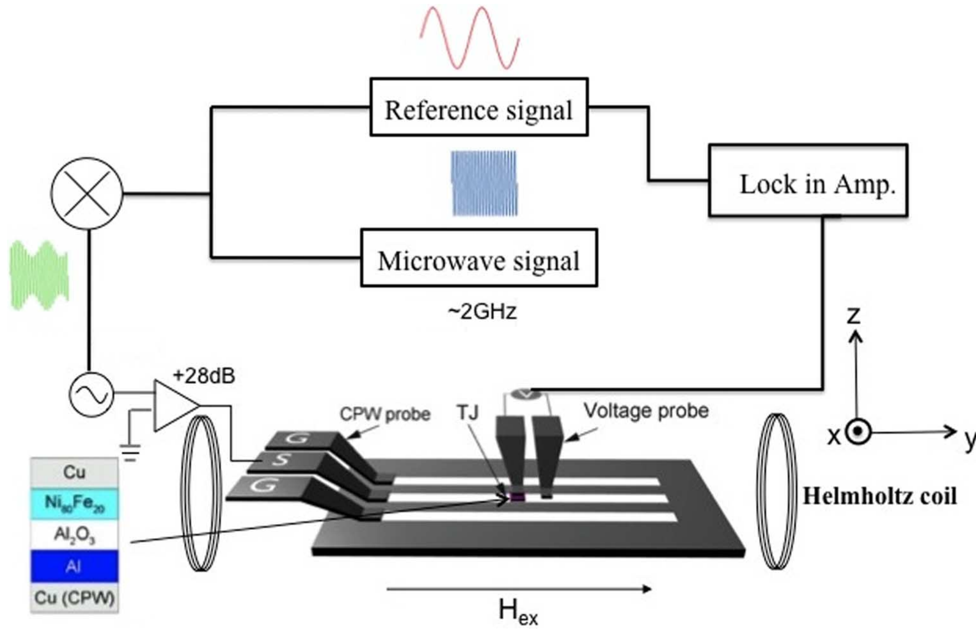

Fig. 3. Schematic diagram of the sample geometry and the experimental setup. The modulated microwave signal is fed into the coplanar waveguide through FPC probe. Tunneling junction is on the top of a signal line and the dc voltage generated across the tunneling junction is measured using a lock-in technique.

$g_\omega = g_\omega^\uparrow + g_\omega^\downarrow$ is the sum of spin-up and spin-down effective conductance at the FM/NM interface. $g_\omega^{\uparrow\downarrow}$ is the real part of the effective spin-mixing conductance, and p_ω is the interfacial spin polarization. Based on this scheme, a direct electrical detection of spin-pumping effect has been realized recently in an $N/F/N$ trilayer [16]. The voltage signals of the order of 100 nV were observed, which is in good agreement with the theory.

Unlike the spin-transfer torque, the spin-pumping effect is not expected in tunneling structures because the spin injection rate is negligibly smaller compared with spin relaxation ration in tunneling structure. Nevertheless, our recent experiment [7] has indicated that more subtle physics concerning the spin and charge pumping occur in tunneling structures, which appears to be very different from $N/F/N$ structures.

In an experiment involving nanometer-thick tunneling junction structure and microwave, how efficient microwave power can be coupled into the tunneling junction becomes a challenge. We chose coplanar waveguide (CPW) to solve this problem because the planar structure is advantageous in terms of the device integration for possible spin-pumping applications, and the dimension of CPW also fits tunneling junctions. The sample geometry and the experimental setup are illustrated in Fig. 3. The tunneling junction was directly fabricated on the top of the CPW signal line. The underlying CPW of 50 Ω characteristic impedance was also designed to avoid the impedance mismatch with the rf probes. The tunneling junction structure is Si/SiO_2/Cu 100/Al 10/AlO_x2.3/$Ni_{80}Fe_{20}$20/Cu 70/Au 25. It was fabricated using magnetron sputtering deposition and the AlO_x tunnel barrier was formed by *in situ* plasma oxidation. After the deposition, two steps of microfabrication were performed. The CPW structures made from the bottom 100-nm Cu layer were formed at the first step and the tunneling junction pillars with the size of 50×50 μm^2 were fabricated on top of the center CPW signal line after the second step. The resistance of the tunneling junction pillar was about 67 kΩ. A microwave signal from an Agilent 8753B vector network analyzer was fed into the CPW and generated a microwave magnetic field $h_{\rm rf}$ along the x-axis in the plane of the tunneling junction. A Helmholtz coil was used to apply a dc magnetic field up to 120 Oe along the CPW (y-axis). The magnetization thus mainly precesses along the y-axis. The voltage across the tunneling junction was measured by contacting a Cascade FPC probe on top of the tunneling junction and the CPW signal line. The microwave frequency varies from 0.7 to 4 GHz with power up to 25 dBm. The microwave amplitude was modulated with a sinusoidal signal of several hundred hertz provided by a function generator in order to allow the use of a lock-in detection technique.

Fig. 4(a) shows the measured dc voltage as a function of the external static magnetic field for an Al/AlO_x/$Ni_{80}Fe_{20}$/Cu tunneling junction. The symmetrical peaks appear at both positive and negative fields at all microwave frequencies and the magnitude of the peaks is of the order of μV, one order larger than the reported value for $N/F/N$ structure [16]. The peak position as a function of the microwave frequency can be well fitted by the Kittel formula yielding parameters consistent with those of $Ni_{80}Fe_{20}$. This result indicates that the voltage peaks are strongly correlated to the ferromagnetic resonance (FMR) of the $Ni_{80}Fe_{20}$ layer. The frequency and the precession angle dependence of the dc voltage are shown in Fig. 4(b). The linear relation between ΔV and the frequency is evident. The precession angle θ under the microwave excitation is estimated from $\Delta R/R \propto (1 - \cos\theta)$ where the TMR changes were measured in IrMn/$Fe_{70}Co_{30}$/AlO_x/$Ni_{80}Fe_{20}$ MTJ under an electrical bias of 20 mV [37]. Although the voltage signal is clear from FMR excitation in $Ni_{80}Fe_{20}$ layer, other possible sources like electrical rectification effect must be eliminated before a qualitative description can be given. The simple structure of $F/I/N$ tun-

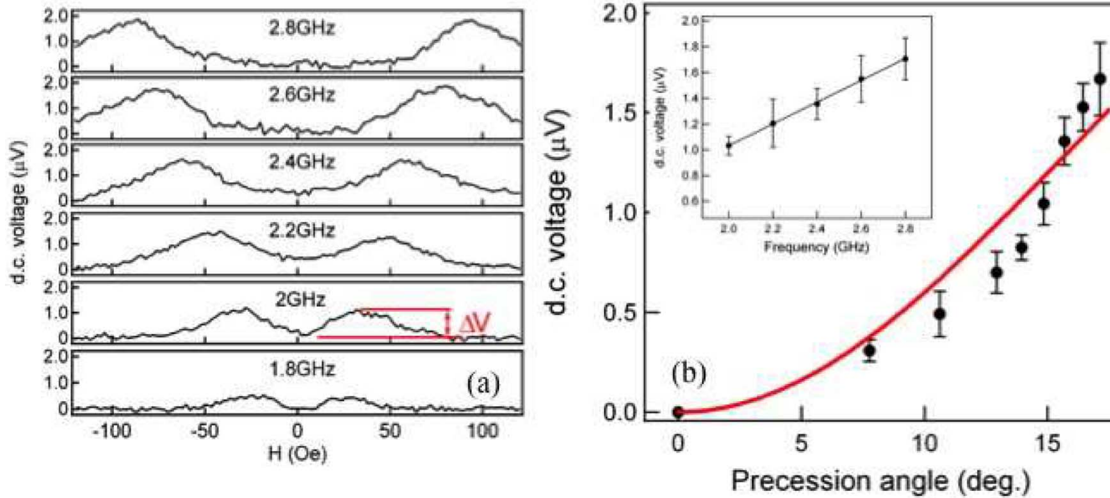

Fig. 4. (a) The dc voltage generated across the Al/AlO_x/$Ni_{80}Fe_{20}$/Cu tunneling junction as a function of the external static magnetic field. (b) The frequency of the microwave field varies from 1.8 to 2.8 GHz. The dc voltage ΔV as a function of the precession angle with the solid line being the fitting using (2). The inset in (b) shows the voltage as a function of the frequency at 10-dBm microwave power.

neling junction makes it naturally immune to the TMR rectification effect since there is only one single ferromagnet. Although the time-dependent anisotropy magnetoresistance (AMR) and the anomalous Hall effect (AHE) could exist, the analysis of our measurement geometry indicates that no dc voltage component could be generated across the junction by those two effects [7]. Thus, no dc voltage generated due to the rectification effect is expected in our tunneling junction under designed measurement geometry. Further investigation in Al/$Ni_{80}Fe_{20}$/Cu and Cu/AlO_x/Al/$Ni_{80}Fe_{20}$/Cu structures also supports the fact that the voltage across the Al/AlO_x/$Ni_{80}Fe_{20}$/Cu tunneling junction was indeed from the AlO_x/$Ni_{80}Fe_{20}$ interface.

At the first glance, the results in Fig. 4(b) can be well fitted with (2). However, the extracted parameters are not physically reasonable. The linear fitting of ΔV versus the frequency in the inset of Fig. 4(b) gives rise to $g_\omega^{\uparrow\downarrow}/g_\omega \approx 6.1$ at a precession angle of 17°, which is too large compared to the estimated value of 0.5 for tunneling contacts [38]. While $\eta_N \approx 0$ is required to fit our precession angle-dependence data, this is impossible in tunneling junction considering the fact that the conductance of a nonmagnetic layer g_N should be several orders of magnitude larger than the effective spin-mixing conductance $g_\omega^{\uparrow\downarrow}$ at F/I interface. All these discrepancies originated from the fact that the standard spin-pumping theory is developed to treat multilayer of ohmic interfaces. From this theory, the spin-pumping effect is never expected in tunneling junction structure where the conductance mismatch at the F/I interface impedes the charge current flowing, thus destroying the pumped spin current. Our results suggest that more complex underlying physics exist in tunneling junction structure. One possible mechanism is the spin charge coupling at the F/I interface [17]. A large voltage in the order of 1–100 μV is predicted by considering the electron–electron interaction, because of the huge difference of the scales associated with the charge screening length (≈ 1 Å) and the spin diffusion length (≈ 100 Å).

Although $F/I/N$ junction is a good candidate to study the spin dynamics and related dc voltage generation because of its simplicity involving only single ferromagnet, $F/I/F$ junction could provide richer physics and potentially more functionalities. The dc voltage generation across $F/I/F$ was expected to be a function of the relative magnetization orientation in two ferromagnets [17], [39]. Fig. 5 shows our experimental results in $F/I/F$ MTJs. The MTJ consists of Cu 100/Ir_{24} Mn_{76}15/$Fe_{30}Co_{70}$6/Al_2 $O_3$2.3/$Ni_{80}Fe_{20}$20/Cu 70. A fast annealing at 180 °C was required to form the exchange pinning on $Fe_{30}Co_{70}$ layer. Parallel (P state) and antiparallel magnetization states (AP state) were then well defined in $F/I/F$ junctions. In the range of the external static magnetic field we used, only the magnetization of NiFe layer was excited to coherently precess under FMR.

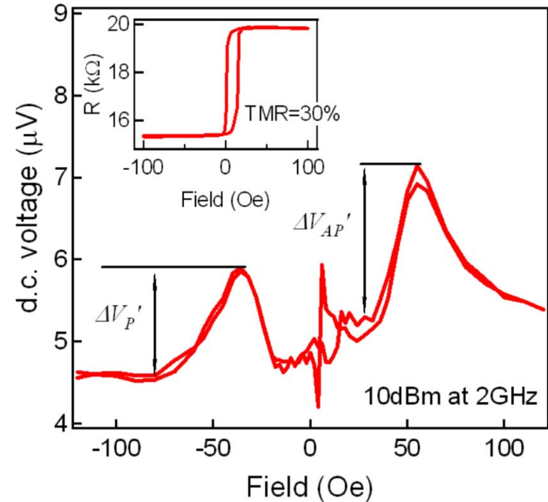

Fig. 5. The dc voltage generated across the Si/SiO_2/Cu/IrMn/CoFe/AlO_x/NiFe/Cu/Au MTJ as the function of the external static magnetic field. The microwave frequency and power are 2 GHz and 10 dBm, respectively. V_P and V_{AP} are voltages in parallel and antiparallel states of MTJ at ferromagnetic resonance. TMR curve in absence of a microwave is shown in the inset.

The TMR, in the absence of microwave input, is shown in the inset of Fig. 5. The TMR is 30% in our junctions, which is normal for amorphous AlO_x barrier-based MTJ. The well-defined two resistance regimes indicate well-defined parallel and

antiparallel magnetization states between two ferromanets. The voltage generated across the CoFe/AlO_x/NiFe junction at 2 GHz is of the order of few μVs, comparable to the ones we obtained in Al/AlO_x/NiFe junction. Unlike $F/I/N$ junction with only a single ferromagnet and symmetric voltage in positive and negative field, the voltages are different corresponding to different magnetization configuration, i.e., $\Delta V_P < \Delta V_{AP}$. A background voltage around 4.5 μV is also seen in Fig. 5, which is due to the microwave electric field.

Because of the complexity of the spin and charge pumping in MTJs, it is very difficult to quantitatively analyze the experiment data. Recently, we proposed a simple theoretical formalism to address the spin pumping and induced voltages by high-frequency spin dynamics in $F/I/N$ and $F/I/F$ junctions using a nonequilibrium Green function approach (NEGF) [18]. Since NEGF formalism takes a microscopic Hamiltonian as an input, it is possible to include the real geometry [40] of experimental devices and the properties of the tunneling barrier, as well as the interactions responsible for spin flip processes in F. Our formalism can yield a remarkably clean physical picture of the spin and charge pumping in ferromagnetic multilayer structures. It consists of 1-D model of spin pumping where a single spin precessing with frequency ω and a neighboring tunneling barrier of height ε_I is attached to the lead. In a rotating frame, the original device is mapped into a four-terminal dc circuit using NEGF. The sample with time-dependent spin interactions is attached to four electrodes that only selectively allow the propagation of one spin species. This picture then can be solved by multi-terminal Landauer–Büttiker-type formulas for spin and charge current.

The detailed discussion of our theoretical formalism can be found in [18]. The calculation provides many useful results and is able to describe the important features observed in our experiment. However, the calculation in work[18] did not include the possible electric bias due to the microwave electric field, which gives a voltage background in all our results. Without this bias, the calculation also yields opposite voltage polarity for ΔV_P and ΔV_{AP}. Here, the electric bias of $\hbar\omega/2$ was incorporated into our formalism according to the real experiment condition. Fig. 6 shows the calculated dc-pumping voltage in $F/I/F$ structures. It should be emphasized that the calculated voltage is at 20 GHz (for easier comparison with other theoretical results at 20 GHz), which can be easily scaled to any frequency since the voltage is linearly proportional to the frequency. The dc voltages V_P and V_{AP} as a function of the barrier height show similar trends compared to the calculations without bias, but the magnitudes of the voltages are both shifted to higher values. Further calculations indicate that the effect of the electric bias is to shift the voltage by the same amount in both parallel and antiparallel states. The background can thus be eliminated by taking $\Delta V = V_{AP} - V_P$, which is on the order of μV at 2 GHz, consistent with our experiment results. As we already mentioned, the standard scattering theory that only considers the spin pumping at F/I interface has difficulty to quantitatively describe either $F/I/N$ or $F/I/F$ structures. The fact that spin pumping is always coupled with the charge has been ignored. In $F/I/F$ junction, the pumped spin current is indeed very small crossing the tunneling barrier. However, the spin current is much enhanced

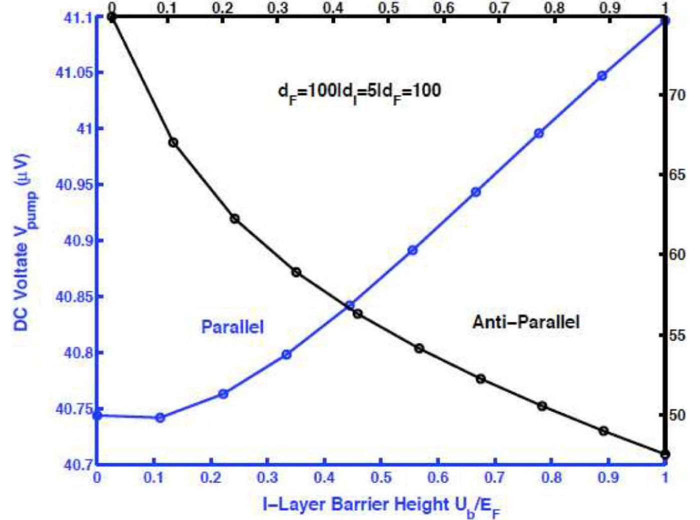

Fig. 6. The dc-pumping voltage in $F/I/F$ multilayer attached to two semi-infinite N electrodes as the function of the barrier height U_b relative to Fermi energy. The precessing cone angle of the magnetization is $\theta = 10^\circ$ and the frequency is $f = 20$ GHz. The structure is under an electric bias of $\hbar\omega/2$.

(more than two folders) in the opposite direction away from the barrier compared with that in a simple F/N structure. This may arise from the quantum interference. The spin current is finally filtered into charge current by the second ferromagnet to generate a pumping voltage across the junction at the order of μV. Both spin and charge contributed to the voltage generation in $F/I/F$ junction, and the voltage is intrinsically much larger than the voltage observed in ohmic F/N structures.

III. Summary

In summary, we have performed a systematic study on the structural evolution under rapid thermal annealing and its corresponding transport properties in MgO-based MTJs. The results clearly indicate high TMR value can be achieved by annealing MTJs at a very short time and at high temperature, and it is directly related to the formation of (001) crystalline structures. The spin dynamics in tunneling structures was also studied through direct electrical detection. A surprisingly large voltage generation in $F/I/N$ and $F/I/F$ junctions was observed, which is contradictory to the prediction from the standard spin-pumping theory. We proposed a theoretical formalism to study spin-pumping effects in ferromagnetic multilayer structures. The formalism can yield a remarkably clean physical picture of the spin and charge pumping in MTJs.

Acknowledgment

This work was supported by DOE DE-FG02-07ER46374.

References

[1] M. N. Baibich, J. M. Broto, and A. Fert, *Phys. Rev. Lett.*, vol. 61, pp. 2472–2475, 1988.

[2] G. Binasch, P. Grunberg, and F. Saurenbach, *Phys. Rev. B, Condens. Matter*, vol. 39, pp. 4828–4830, 1989.

[3] I. Žutić, J. Fabian, and S. Das Sarma, "Spintronics: Fundamentals and applications," *Rev. Modern Phys.*, vol. 76, p. 323, 2004.

[4] K. I. Lee, S. J. Joo, J. H. Lee, K. Rhie, T.-S. Kim, W. Y. Lee, K. H. Shin, B. C. Lee, P. LeClair, J.-S. Lee, and J.-H. Park, "Kondo effect in magnetic tunnel junctions," *Phys. Rev. Lett.*, vol. 98, 2007, 107202.

[5] H. Saito, S. Yuasa, and K. Ando, "Origin of the tunnel anisotropic magnetoresistance in $Ga_{1-x}Mn_xAs/ZnSe/Ga_{1-x}MnxAs$ magnetic tunnel junctions of II-VI/III-V heterostructures," *Phys. Rev. Lett.*, vol. 95, 2005, 086604.

[6] M. Bowen, A. Barthélémy, M. Bibes, E. Jacquet, J.-P. Contour, A. Fert, F. Ciccacci, L. Duò, and R. Bertacco, "Spin-polarized tunneling spectroscopy in tunnel junctions with half-metallic electrodes," *Phys. Rev. Let.*, vol. 95, 2005, 137203.

[7] T. Moriyama, R. Cao, X. Fan, G. Xuan, B. K. Nikolic, Y. Tserkovnyak, J. Kolodzey, and J. Q. Xiao, "Tunnel barrier enhanced voltage signal generated by magnetization precession of a single ferromagnetic layer," *Phys. Rev. Lett.*, vol. 100, 2008, 067602.

[8] S. Yuasa, T. Nagahama, A. Fukushima, Y. Suzuki, and K. Ando, "Giant room-temperature magnetoresistance in single-crystal Fe/MgO/Fe magnetic tunnel junctions," *Nature Mater.*, vol. 3, pp. 868–871, Dec. 2004.

[9] S. S. P. Parkin, C. Kaiser, A. Panchula, P. M. Rice, B. Hughes, M. Samant, and S. H. Yang, "Giant tunnelling magnetoresistance at room temperature with MgO (100) tunnel barriers," *Nature Mater.*, vol. 3, pp. 862–867, Dec. 2004.

[10] S. Yuasa and D. D. Djayaprawira, "Giant tunnel magnetoresistance in magnetic tunnel junctions with a crystalline MgO(001) barrier," *J. Phys. D, Appl. Phys.*, vol. 40, pp. R337–R354, Nov. 7, 2007.

[11] J. C. Sankey, Y. T. Cui, J. Z. Sun, J. C. Slonczewski, R. A. Buhrman, and D. C. Ralph, "Measurement of the spin-transfer-torque vector in magnetic tunnel junctions," *Nature Phys.*, vol. 4, pp. 67–71, Jan. 2008.

[12] C. Heiliger, M. Gradhand, P. Zahn, and I. Mertig , "Tunneling magnetoresistance on the subnanometer scale," *Phys. Rev. Lett.*, vol. 99, 2007, 066804.

[13] S. Kaka, M. R. Pufall, W. H. Rippard, T. J. Silva, S. E. Russek, and J. A. Katine, "Mutual phase-locking of microwave spin torque nano-oscillators," *Nature*, vol. 437, pp. 389–392, 2005.

[14] M. Julliere*, Phys. Lett. A*, vol. 54, p. 225, 1975.

[15] A. Brataas, Y. Tserkovnyak, G. E. W. Bauer, and B. I. Halperin*, Phys. Rev. B, Condens. Matter*, vol. 66, 2002, 060404.

[16] M. V. Costache, M. Sladkov, S. M. Watts, and C. H. van der Wal*, Phys. Rev. Lett.*, vol. 97, 2006, 216603.

[17] S. T. Chui and Z. F. Lin*, Phys. Rev. B, Condens. Matter*, vol. 77, 2008, 094432.

[18] S.-H. Chen, C.-R. Chang, J. Q. Xiao, and B. K. Nikolic*, Phys. Rev. B, Condens. Matter*, vol. 79, 2009, 054424.

[19] W. H. Butler, X.-G. Zhang, T. C. Schulthess, and J. M. MacLaren, "Spin-dependent tunneling conductance of Fe/MgO/Fe sandwiches," *Phys. Rev. B, Condens. Matter*, vol. 63, 2001, 054416.

[20] J. Mathon and A. Umerski, "Theory of tunneling magnetoresistance of an epitaxial Fe/MgO/Fe(001) junction," *Phys. Rev. B, Condens. Matter*, vol. 6322, Jun. 1, 2001, 220403.

[21] D. D. Djayaprawira, K. Tsunekawa, M. Nagai, H. Maehara, S. Yamagata, N. Watanabe, S. Yuasa, Y. Suzuki, and K. Ando, "230% room-temperature magnetoresistance in CoFeB/MgO/CoFeB magnetic tunnel junctions," *Appl. Phys. Lett.*, vol. 86, 2005, 092502.

[22] S. Ikeda, J. Hayakawa, Y. Ashizawa, Y. M. Lee, K. Miura, H. Hasegawa, M. Tsunoda, F. Matsukura, and H. Ohno*, Appl. Phys. Lett.*, vol. 93, 2008, 082508.

[23] Y. S. Choi, Y. Nagamine, K. Tsunekawa, H. Maehara, D. D. Djayaprawira, S. Yuasa, and K. Ando, "Effect of Ta getter on the quality of MgO tunnel barrier in the polycrystalline CoFeB/MgO/CoFeB magnetic tunnel junction," *Appl. Phys. Lett.*, vol. 90, 2007, 012505.

[24] Y. M. Lee, J. Hayakawa, S. Ikeda, F. Matsukura, and H. Ohno, "Giant tunnel magnetoresistance and high annealing stability in CoFeB/MgO/CoFeB magnetic tunnel junctions with synthetic pinned layer," *Appl. Phys. Lett.*, vol. 89, 2006, 042506.

[25] T. Moriyama, C. Ni, W. G. Wang, X. Zhang, and J. Q. Xiao, "Tunneling magnetoresistance in (001)-oriented FeCo/MgO/FeCo magnetic tunneling junctions grown by sputtering deposition," *Appl. Phys. Lett.*, vol. 88, 2006, 222503.

[26] Y. Z. Liu, W. G. Wang, T. Moriyama, J. Q. Xiao, and Z. Zhang, "Direct measurement of barrier asymmetry in AlOx/ZrOy magnetic tunnel junctions using off-axis electron holography," *Phys. Rev. B, Condens. Matter*, vol. 75, 2007, 134420.

[27] W. G. Wang, C. Ni, A. Rumaiz, Y. Wang, X. Fan, T. Moriyama, R. Cao, Q. Y. Wen, H. W. Zhang, and J. Q. Xiao, "Real-time evolution of tunneling magnetoresistance during annealing in CoFeB/MgO/CoFeB magnetic tunnel junctions," *Appl. Phys. Lett.*, vol. 92, 2008, 152501.

[28] W. G. Wang, T. Moriyama, R. Cao, and J. Q. Xiao, (unpublished).

[29] E. M. Hankiewicz, G. Vignale, and Y. Tserkovnyak, arXiv:0804.0820.

[30] J. C. Slonczewski*, J. Magn. Magn. Mater.*, vol. 159, p. L1, 1996.

[31] L. Berger*, Phys. Rev. B, Condens. Matter*, vol. 54, p. 9353, 1996.

[32] Y. Tserkovnyak, A. Brataas, and G. E. W. Bauer, "Spin pumping and magnetization dynamics in metallic multilayers," *Phys. Rev. B, Condens. Matter*, vol. 66, 2002, 224403.

[33] Y. Tserkovnyak, A. Brataas, G. E. W. Bauer, and B. I. Halperin, "Nonlocal magnetization dynamics in ferromagnetic heterostructures," *Rev. Modern Phys.*, vol. 77, pp. 1375–1421, 2005.

[34] S. Mizukami, Y. Ando, and T. Miyazaki, "Ferromagnetic resonance linewidth for NM/80NiFe/NM films (NM = Cu, Ta, Pd and Pt)," *J. Magn. Magn. Mater.*, vol. 226, pp. 1640–1642, 2001.

[35] R. Cao, X. Fan, T. Moriyama, and J. Q. Xiao, "Nonlinear effective spin-mixing conductance in $Pt/Ni_{80}Fe_{20}/Pt$ thin films," *J. Appl. Phys.*, vol. 105, 2009, 07C705.

[36] X. Wang, G. Bauer, B. V. Wees, A. Brataas, and Y. Tserkovnyak, "Voltage generation by ferromagnetic resonance at a nonmagnet to ferromagnet contact," *Phys. Rev. Lett.*, vol. 97, 2006, 216602.

[37] T. Moriyama, R. Cao, X. Fan, and J. Q. Xiao, unpublished.

[38] A. Brataas, G. E. W. Bauer, and P. J. Kelly*, Phys. Rep.*, vol. 427, pp. 157–255, 2006.

[39] Y. Tserkovnyak, T. Moriyama, and J. Q. Xiao*, Phys. Rev. B, Condens. Matter*, vol. 78, 2008, 020401(R).

[40] T. Taniguchi and H. Imamura*, Phys. Rev. B, Condens. Matter*, vol. 78, 2008, 224421.